ELSEVIER

Biochimica et Biophysica Acta 1228 (1995) 28–36

BBA Biochimica et Biophysica Acta

Spectroscopic and kinetic characterization of the spinach plastocyanin mutant Tyr83-His: a histidine residue with a high pK value

Kalle Sigfridsson [a], Örjan Hansson [a,*], B. Göran Karlsson [a], Lars Baltzer [b], Margareta Nordling [a], Lennart G. Lundberg [a]

[a] *Department of Biochemistry and Biophysics, Lundberg Laboratory, Göteborg University and Chalmers University of Technology, Medicinaregatan 9C, S-413 90 Göteborg, Sweden*

[b] *Department of Organic Chemistry, Göteborg University and Chalmers University of Technology S-412 96 Göteborg, Sweden*

Received 20 January 1994; accepted 29 September 1994

Abstract

Tyrosine-83 in spinach plastocyanin (Pc) has been modified by site-directed mutagenesis to a histidine. An NMR titration yields a pK value of 8.44 for this residue. The high value is probably due to the acidic residues close to this site. The reduction potential is increased by 35 mV at pH 7.5, but only slightly, if at all, at pH 8.9. EPR and optical absorption bands associated with the copper site are not affected by the mutation, either at pH 7.5 or at pH 8.9. The electron transfer (ET) to Photosystem I (PS I), as studied by a flash-photolysis technique, is pH dependent for the mutant, being slower than the wild type at pH 7.5 but more similar to it at pH 8.9. The data have been interpreted with a model that includes a rate-limiting conformational change in the Pc-PS I complex which precedes the intracomplex ET (Bottin, H. and Mathis, P. (1985) Biochemistry 24, 6453–6460). The slower kinetics at the lower pH for the mutant is attributed to a dual effect of the protonation of the His-83 residue: (i) A destabilization of the 'close' bound conformation, i.e., the one competent in electron transfer, and (ii) a smaller intracomplex ET rate constant, partly due to a smaller driving force for ET. From this it is concluded that the Tyr-83 residue is not a part of the ET pathway to PS I.

Keywords: Electron transfer; Flash photolysis; NMR; Photosynthesis; Photosystem I; Site-directed mutagenesis

1. Introduction

Plastocyanin (Pc) is a small, blue copper protein which acts as an electron carrier between the cytochrome b_6f and Photosystem I (PS I) complexes in the photosynthetic electron transfer (ET) chain. The photooxidized reaction-center chlorophyll P700 in PS I is reduced by Pc and the oxidized Pc is in turn reduced by cytochrome f (reviewed in [1]).

Two areas on the surface of Pc were identified as being of importance in the ET reactions already when the three-dimensional structure was first reported [2]. One is the hydrophobic patch around the copper ligand His-87, and the other is an acidic patch around Tyr-83. These regions are also referred to as the adjacent and remote sites, respectively [3]. Support for this suggestion has come from studies of chemically modified Pc and of the reactivity between Pc and low-molecular weight complexes (reviewed in [3]).

In order to further elucidate the role of particular amino-acid residues, site-specific mutations were recently introduced in the structural gene for Pc from spinach [4,5] and pea [6]. For one mutant, where Leu-12 in the hydrophobic patch is replaced with a Glu residue, the ET to PS I was found to be much slower than for the wild type, suggesting an important role for this region in the interaction with PS I [4]. This was further supported by the findings that replacement of Gly-10 and Ala-90 in the hydrophobic patch with Leu also result in a strong impairment of the reaction with PS I [5]. On the other hand,

Abbreviations: ET, electron transfer; P, P700, reaction-center chlorophyll; Pc, plastocyanin; PS I, Photosystem I.

* Corresponding author. E-mail: orjan@bcbp.gu.se. Fax: +46 31 7733910.

SSDI 0005-2728(94)00158-8

studies of Leu- and Phe-mutations of Tyr-83 suggest a crucial role for this residue in the reaction with cytochrome *f* [6].

A straightforward interpretation of the mutant studies would be that Pc employs different pathways in the reactions with its redox partners, Tyr-83 in the acidic patch when accepting electrons from cytochrome *f* and His-87 in the hydrophobic patch when donating electrons to PS I. The situation is, however, not entirely clear. For example, in the case of cytochrome *f*, a Leu12-Asn plastocyanin mutant showed a marked increase in binding constant while the kinetics of reduction of an Asp42-Asn mutant were not significantly different from wild type, despite the loss of a negative charge in the acidic patch [7]. With regards to the reaction with PS I, a Tyr83-Leu mutant from spinach displayed altered ET kinetics [5] while the same mutation of Pc from pea did not (He, S., Sigfridsson, K., Modi, S., Bendall, D.S., Hansson, Ö. and Gray, J.C., unpublished observations).

In the present work, special attention is paid to a Tyr83-His mutant of spinach Pc (hereafter denoted Pc(Y83H)). This mutant displayed a significantly higher reduction potential than the wild type (Pc(WT)), as well as a markedly slower ET reaction with PS I at pH 7.5 [4]. The possible cause for this behavior has now been examined in detail. The increase in reduction potential is found to be due to an influence from the protonated form of His-83. The reduction potential is decreased by approx. 30 mV upon deprotonation of this residue. These results are in qualitative agreement with those obtained from kinetic studies of the reactivity of Pc(Y83H) with inorganic redox partners [8].

The earlier studies of the PS I reaction have been extended to include the effect of varying Pc concentrations and elevated pH. The data are interpreted in terms of a model that includes a rate-limiting conformational change in the Pc-PS I complex which precedes the intracomplex ET. This model, originally proposed by Bottin and Mathis [9], accounts better for the kinetics than the simple model used in the previous work [4]. For the Pc(Y83H) mutant, it is found that the details of the ET kinetics depend critically on the protonation state of the His-83 residue.

2. Materials and methods

2.1. Preparation of Pc and PS I

Recombinant wild-type plastocyanin and the Pc(Y83H) mutant were prepared using the previously described system for overexpression of Pc in *E. coli* [10] employing the expression vector pUG101t$_r$ [4]. The mutant protein was constructed using polymerase chain reaction (PCR) amplification according to the method of Landt et al. [11] with the modifications described in [4]. After mutagenesis the entire gene of the mutant protein was sequenced and found to be correct. Growth and fractionation of *E. coli* cells and purification of Pc was made as in [4] with the following exceptions. The bacterial strain used was *E. coli* RV308 (ATCC 31608) [12]. A Sepharose HP(26/10) (Pharmacia) FPLC column was used in the last ion-exchange chromatography and an ordinary Sephacryl S-100 column was used in the final gel-filtration step. The buffer was changed to 20 mM Tris-HCl (pH 7.5 or pH 8.9) during the gel filtration. The Pc-containing fractions after each of these steps were pooled and concentrated by dialysis against dry polyethylene glycol. The absorbance ratio A_{278}/A_{597} was 1.1 for Pc(Y83H). The concentration of holo-Pc was determined spectrophotometrically under oxidizing conditions using an absorption coefficient of 4900 $M - 1cm^{-1}$ at 597 nm [13].

Digitonin-solubilized PS I particles (D-144 particles) with 240 chlorophyll/P700 were prepared from spinach according to [14]. The particles were suspended in 20 mM Tris (pH 7.5) and stored at 77 K until use.

2.2. Redox titration of Pc

The reduction potential of Pc was determined by spectrophotometric titration in 20 mM Tris at pH 7.5 and 8.9. For measurements at pH 8.9, enough NaCl was added to give an ionic strength equal to the one at pH 7.5. The reduction potentials obtained are summarized in Table 1. The values for Pc(WT) are similar to previously reported values, which range from 370 [13] to 382 mV [15].

Table 1
Reduction potentials and parameters describing the electron transfer to Photosystem I for wild-type and Tyr83-His plastocyanin mutants

Plastocyanin	pH	E^0 (mV)	k_1 (10^3 s^{-1})	k_{2max} (10^3 s^{-1})	C_{k2} (μM)	R_{max}	C_R (μM)
Wild type	7.5	384	74	19	52	0.74	36
Wild type	8.9	388	75	20	88	0.65	40
Tyr83-His	7.5	419	41	7	24	0.37	35
Tyr83-His	8.9	390	51	12	41	0.53	37

The reduction potential (E^0) was determined in 20 mM Tris (pH 7.5 or 8.9) by monitoring the 597 nm absorbance as the ratio of (potassium) ferricyanide to ferrocyanide was varied. The kinetic parameters were obtained from analysis of flash-induced absorption changes of P700 under the same conditions as for Fig. 4 but using a range of plastocyanin concentrations. k_1 is the average value of the apparent rate constant of the fast phase. k_{2max} and R_{max} are the saturating values of the apparent rate constant of the intermediary phase and of the fraction of the fast phase in the P700 decay kinetics. C_{k2} and C_R are the plastocyanin concentrations at which half the saturating values are obtained.

2.3. NMR spectroscopic pH titrations

Pc(Y83H) was transferred to 20 mM sodium phosphate (pH 6.4) in D_2O, and brought to a final Pc concentration of 1 mM. Small amounts of dithionite in 0.1 M NaOD was used to reduce the protein. NaOD and DCl (0.1 M and 1.0 M) were used for pH adjustments and pH and pK values quoted (as pH* and pK*) refer to direct meter readings without correction for the deuterium isotope effect. Due to the experimental procedure the ionic strength varied between approx. 40 to 60 mM.

A Varian Unity 500 MHz NMR spectrometer with an inverse detection probe was used to collect 64 transients at each pH* value at 25°C. The acquisition time was 1 s and the sweep width 8 kHz. The data were zero-filled from 16 to 32 kbyte and a line-broadening factor of 1 Hz was applied before Fourier transformation. Difference spectroscopy was used to follow the titration of the His-83 residue. The titration parameters were obtained by non-linear least-squares curve-fitting of the NMR data to a sigmoidal curve. The line broadening was measured in spectra that had only been zero-filled before the Fourier transformation.

2.4. Optical absorption and EPR spectroscopy

The Pc(WT) and Pc(Y83H) mutant were investigated spectroscopically at pH 7.5 and 8.9 for a possible influence of the mutation or the pH on the electronic structure of the copper site. No effects were, however, discernible from the visible absorption or EPR spectra. The parameters obtained for the low-field part of the EPR spectrum, $g_{\|} = 2.24$ and $A_{\|} = 6.4$ mT, agree with the values for Pc prepared from spinach [16]. Optical spectra were obtained at room temperature with a Shimadzu UV-160A spectrophotometer. EPR spectra were recorded at 11 K with a Bruker ER 200D-SRC spectrometer operating at 9.4 GHz and equipped with an Oxford Instruments ESR-9 helium-flow cryostat.

2.5. Kinetic methods

The kinetics of the ET from Pc to PS I were studied by monitoring the flash-induced absorption changes at 830 nm due to oxidized P700. Pc in 20 mM Tris (pH 7.5 or 8.9) was mixed with PS I to a final chlorophyll concentration of 0.9 mg/ml. Sodium ascorbate (2 mM) and methyl viologen (0.1 mM) were added in order to reduce Pc and oxidize the PS I acceptor side, respectively, between the flashes (spaced 20 s apart). $MgCl_2$ (7 mM at pH 7.5 and 9 mM at pH 8.9) was added to give a final ionic strength of 38 mM. The ET from Pc to PS I is known to be facilitated by millimolar concentrations of $MgCl_2$ in this type of digitonin-solubilized PS I particles [17,18]. From studies at different $MgCl_2$ concentrations it was found that the concentrations given above resulted in an optimal binding of Pc to PS I.

The experimental setup was essentially as described in [19]. Excitation of PS I was obtained by short (10 ns) flashes (532 nm) from a Nd:YAG laser. Photooxidation and reduction of P700 was monitored at 830 nm with a continuous wave diode laser using an silicium photodiode (UDT PIN-10D) connected to a home-built amplifier (gain, 50; bandwidth, 8 Hz to 30 MHz). The diode laser was driven with a Melles Griot 06DLD203 unit. Acquisition of the transient absorption signals and fitting of the signals to a sum of exponentials was made as previously described [19]. Other experimental conditions are given in the figure legends.

3. Results

3.1. NMR titration of Pc(Y83H)

The ^{1}H-NMR spectrum of the Pc(Y83H) mutant (Fig. 1) is almost identical to the Pc(WT) spectrum (not shown), suggesting very small conformational changes in the mutant protein. The most obvious changes in the Pc(Y83H) spectrum are the disappearance of a signal at 6.52 ppm,

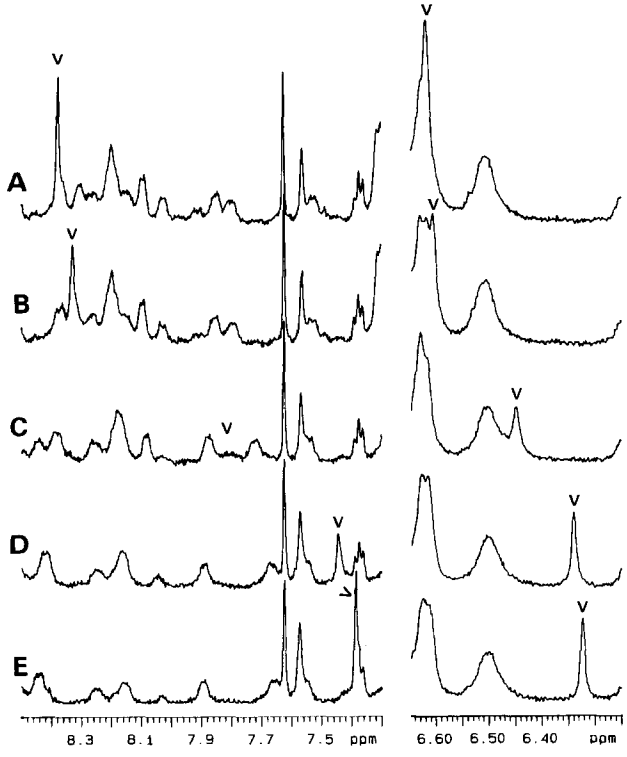

Fig. 1. Effect of pH* on the 500 MHz ^{1}H-NMR spectrum of reduced Pc(Y83H). The figure shows two parts of the aromatic region at pH* values of 7.05 (A), 7.35 (B), 8.50 (C), 9.35 (D) and 9.75 (E). The positions of the His-83 C2H and C4H proton resonances are indicated with a 'V'. The concentration of Pc was 1 mM in 20 mM sodium phosphate in D_2O. The NMR conditions were as described in Section 2. The additional changes in the amide region (above 7.7 ppm) that are observed at the higher pH* values are mainly due to an exchange of ^{1}H for ^{2}H during the titration.

which has been assigned to the Tyr-83 C2,6H protons [20] and thus should be missing, and the presence of two singlet peaks at 6.6 and 8.4 ppm at pH* 6.40. Based on the chemical shift of the new peaks, their pH dependence as well as their inertness to deuterium exchange, these peaks are assigned to the His-83 residue of the mutant protein. The signal at 8.4 ppm is tentatively assigned to C2H ($C_{\epsilon 1}H$) and the signal at 6.6 ppm to C4H ($C_{\delta 2}H$).

The resonance peaks from the His-83 C2H and C4H protons are continuously shifted upfield with increasing pH* (Fig. 2), indicating a rapid exchange with solvent deuterons. A curve-fitting analysis of the data yields a chemical-shift difference, $\Delta\nu_{AB}$, of 543 and 161 Hz for the C2H and C4H protons, respectively, and a pK* value of 8.44 for both data sets. The maximal line broadening of the C4H signal was found to be 4 Hz at a pH* close to pK* (Fig. 3). In the following, the line-broadening data will be used to estimate the deuteron (proton) exchange rate.

Removal of a proton from an acid is generally base-catalyzed, and, for an imidazole (Im), includes both a direct proton dissociation:

$$ImH^+ + H_2O \underset{k_{on}^{H^+}}{\overset{k_{off}^{H^+}}{\rightleftharpoons}} Im + H_3O^+ \quad (1)$$

as well as an attack of hydroxide upon ImH^+ (with a second-order rate constant $k_{on}^{OH^-}$):

$$ImH^+ + OH^- \underset{k_{off}^{OH^-}}{\overset{k_{on}^{OH^-}}{\rightleftharpoons}} Im + H_2O \quad (2)$$

Buffer molecules may contribute in a manner similar to Eq. (2). For buffer-free systems the observed increase in the line broadening, $\Delta\nu_{ex}$, is approximated in the fast-exchange limit by [21]:

$$\Delta\nu_{ex} \approx \frac{4\pi(\Delta\nu_{AB}P_AP_B)^2}{P_Ak_{off}^{H^+} + P_Bk_{off}^{OH^-}} \quad (3)$$

where P_A and P_B denote the fractions of protonated and deprotonated forms of the imidazole, respectively, and $k_{off}^{H^+}$ and $k_{off}^{OH^-}$ are first-order rate constants according to Eqs. (1) and (2), respectively.

It is often assumed that $k_{off}^{H^+} \gg k_{off}^{OH^-}$ for a titrating imidazole. Then it follows from Eq. (3) that the maximal line broadening would appear at $P_A = 1/3$ which, in the present case, would correspond to pH 8.74. However, the maximal line broadening for His-83 in Pc(Y83H) occurs very close to the pK* for the titration, which can happen when $k_{off}^{H^+}$ and $k_{off}^{OH^-}$ are of the same order of magnitude [21]. At the pK*($P_A = P_B = 0.5$) the line broadening is $\Delta\nu_{ex} = 4$ Hz and this, together with $\Delta\nu_{AB} = 161$ Hz, yields an exchange rate $k_{off}^{H^+} + k_{off}^{OH^-} \approx 10^4$ s^{-1} from Eq. (3). Separate values of the two rate constants can be obtained from a fit of the experimental line-broadening data to Eq. (3) at all pH values studied. The best fit was obtained with the rate constants $k_{off}^{H^+} = 3.0 \cdot 10^3$ s^{-1} and $k_{off}^{OH^-} = 7.5 \cdot 10^3$ s^{-1} (Fig. 3).

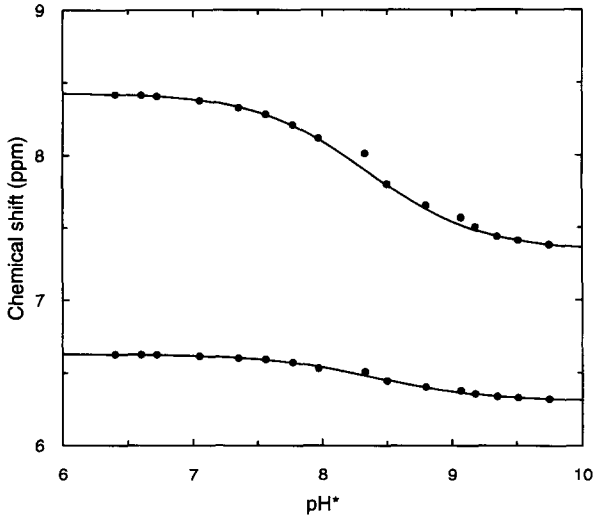

Fig. 2. Effect of pH* on the chemical shift of the His-83 C2H (upper part) and C4H (lower part) proton resonances of reduced Pc(Y83H). The experimental conditions were as in Fig. 1. The solid curves are theoretical fits to the data from which chemical-shift differences, $\Delta\nu_{AB}$, of 543 (C2H) and 161 Hz (C4H) and a pK* value of 8.44 were obtained.

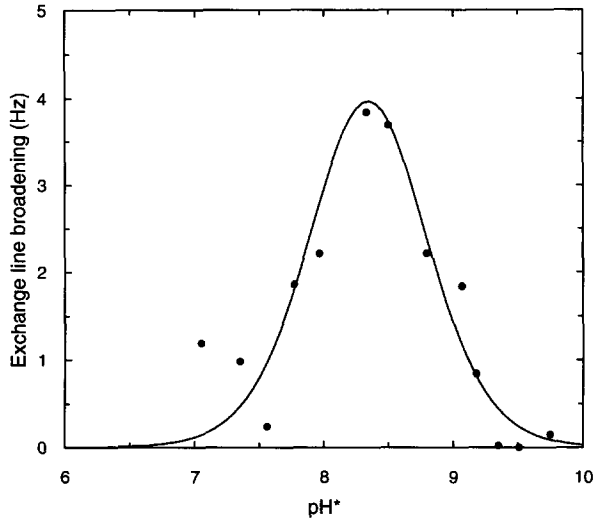

Fig. 3. Effect of pH* on the exchange line-broadening of the C4H proton resonance of reduced Pc(Y83H). The experimental conditions were as in Fig. 1. The solid curve was calculated using Eq. (3) in the text with the following parameters: pK = 8.44, $\Delta\nu_{AB}$ = 161 Hz, $k_{off}^{H+} = 3.0 \cdot 10^3$ s^{-1} and $k_{off}^{OH^-} = 7.5 \cdot 10^3$ s^{-1}.

3.2. Kinetic measurements

The ET from Pc to PS I was investigated for a possible effect of the mutation on the kinetics. As shown in Fig. 4, flash-excitation of a mixture of PS I particles and Pc results in an instantaneous absorption increase at 830 nm (due to photooxidation of P700) followed by a multiphasic decrease (due to reduction of $P700^{ox}$ by Pc^{red}; where

'ox/red' = oxidized/reduced species). At pH 7.5 the decay kinetics for the Pc(Y83H) mutant are slower than for Pc(WT) (Fig. 4A,C). Increasing the pH to 8.9 results in a faster kinetics for Pc(Y83H) (Fig. 4B) while Pc(WT) is unaffected (not shown). The absorption transients have been analyzed with a non-linear least-squares curve-fitting program. At all Pc concentrations studied (20 μM to 1 mM), good fits could only be obtained if the model function consisted of a sum of at least three decaying exponentials (Fig. 4D,E). The amplitudes and apparent first-order rate constants of the exponentials will be denoted by A_i and k_i, $i = 1–3$.

In a first, exploratory step, the transients were subjected to an analysis in which all A_i and k_i, $i = 1–3$, were allowed to vary freely. The result for k_1, the apparent rate constant of the fastest component, is shown in Fig. 5 as a function of Pc concentration for Pc(WT) and Pc(Y83H) at pH 7.5 and 8.9. The large spread in k_1 within each data set reflects the considerable uncertainty that results when this many parameters are fitted. Despite this, it is clear that the estimated k_1 values are independent of the Pc concentration and that k_1 is larger for Pc(WT) than for Pc(Y83H). The k_1 value for the mutant, but not for Pc(WT), increases significantly upon changing the pH from 7.5 to 8.9. The dashed lines in Fig. 5 indicate the average of k_1 for each data set and the average values are also listed in Table 1.

The apparent rate constant of the slowest component, k_3, was also largely independent of the Pc concentration. An average value of 330 s^{-1} was obtained for both Pc(WT) and Pc(Y83H), irrespective of pH.

As will be discussed below, k_1 is largely determined by

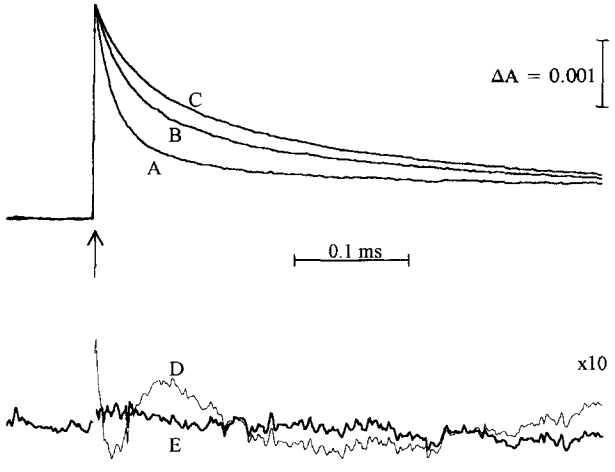

Fig. 4. Flash-induced absorption transients at 830 nm of PS I particles with Pc(WT) at pH 7.5 (A) and with Pc(Y83H) at pH 8.9 (B) and 7.5 (C). Each sample contained PS I particles (0.9 mg chlorophyll/ml), 2 mM sodium ascorbate, 0.1 mM methyl viologen and 1 mM Pc in 20 mM Tris buffer (pH 7.5 or 8.9). $MgCl_2$ was added to a final ionic strength of 38 mM at both pH values. The cuvette (thickness, 1 mm) was placed at 45° to the measuring beam. The traces shown are the averaged effect of 16 flashes spaced 20 s apart. The lower part of the figure shows the residuals obtained from a curve-fitting of trace A to two (D) and three (E) decaying exponentials.

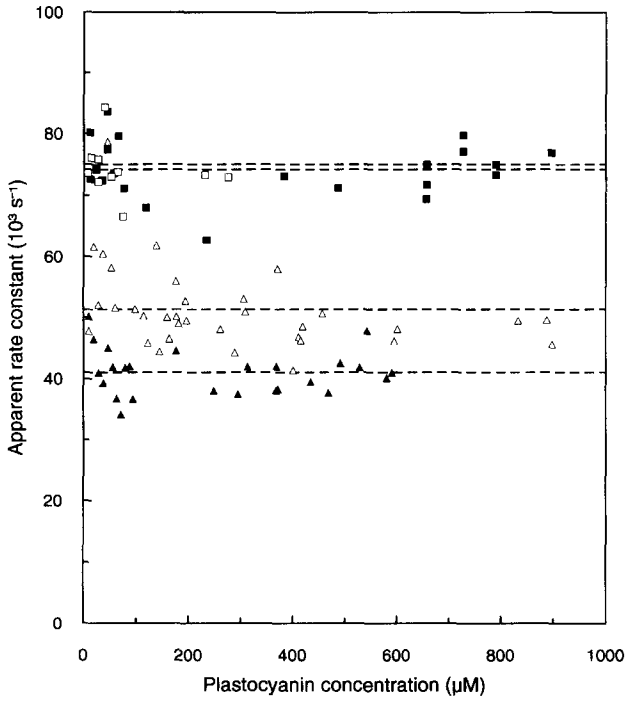

Fig. 5. Apparent rate constant of the fast phase, k_1, in the decay kinetics of oxidized P700 as a function of Pc concentration for Pc(WT) (squares) and Pc(Y83H) (triangles) at pH 7.5 (filled symbols) and 8.9 (open symbols). The experimental conditions were as in Fig. 4. k_1 was obtained from a curve-fitting analysis of the absorption transients using a model function that consisted of a sum of three decaying exponentials. All three amplitudes and rate constants were allowed to vary freely until a best fit was achieved. The average values of k_1 are indicated by dashed lines.

k_{et}, the rate constant for the intracomplex ET from Pc to P700. Thus, the k_1 values in Table 1 indicate that k_{et} is different for the Pc(Y83H) mutant. The change is towards a smaller rate constant which is in qualitative agreement with the reduced driving force for ET from Pc to P700. The reduction potential, E^0, of P700 is 0.49 V for this preparation, independent of pH [4,22]; E^0 for Pc(WT) and Pc(Y83H) are given in Table 1. The increase in k_1 with pH for the mutant is also largely as expected, since E^0 for Pc(Y83H) decreases with pH, resulting in a larger driving force at pH 8.9.

More quantitative conclusions about the ET kinetics require a consideration of the other decay components. In a second step of the analysis, all absorption transients were again subjected to a curve-fitting procedure, but now with k_1 fixed at the values listed in Table 1 and k_3 fixed at 330 s^{-1}. This procedure resulted in a much less spread in the remaining free parameters k_2, A_1, A_2 and A_3. The estimated k_2 values are displayed in Fig. 6, and Fig. 7 shows the relative contribution of the fast phase to the decaying kinetics, defined as the amplitude ratio $R = A_1/(A_1 + A_2)$. Both k_2 and R saturate at high Pc concentrations, as has been noted previously [9]. In order to describe the saturation quantitatively, k_2 and R were fit to hyperbolic functions $k_{2max}[Pc]/(C_{k2} + [Pc])$ and $R_{max}[Pc]/(C_R + [Pc])$,

where k_{2max} and R_{max} denote the saturating values and C_{k2} and C_R are the Pc concentrations at which half the saturating levels are reached. These descriptive parameters are listed in Table 1. Evidently, the mutation has resulted in decreased values for all these parameters except C_R, which remains at the Pc(WT) value of 35–40 μM.

The amplitude A_3 of the slowest, millisecond, component was found to be constant at about 20% of the total initial amplitude at Pc concentrations above 200 μM in all four data sets. Since the absorption coefficient of Pc^{ox} at 830 nm is 18% of that of $P700^{ox}$, it is reasonable to ascribe this component to the reduction of Pc^{ox} by ascorbate [4,9]. This reaction is expected to take place in the seconds range and the true rate constant is therefore obscured by the low-frequency cut-off of the AC amplifier (8 Hz). The remaining two components are ascribed to the decay kinetics of $P700^{ox}$.

At Pc concentrations below 200 μM there was an increase in A_3 with decreasing Pc concentration at the expense of the two faster components. Since the amplitude of the signal from Pc^{ox} is expected to remain constant (at 18% of the total initial amplitude) this means that an additional, third, component appears in the $P700^{ox}$ decay kinetics at low Pc concentrations. Fits with four decaying exponentials (three submillisecond and one millisecond component) were, however, found to be unreliable. The following analysis will therefore only be based on the data from the high Pc concentration range (> 200 μM), where a three-component fit was sufficient.

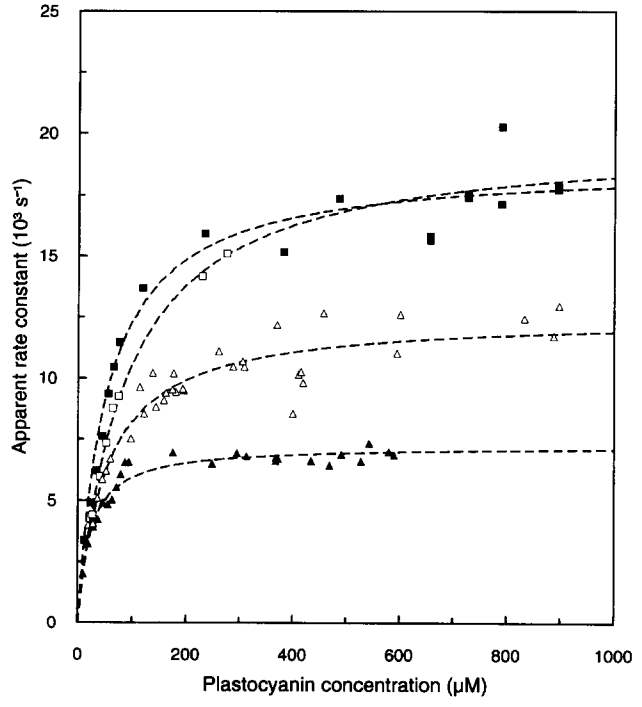

Fig. 6. Effect of Pc concentration on the apparent rate constant of the intermediary phase, k_2, in the decay kinetics of oxidized P700 for Pc(WT) (squares) and Pc(Y83H) (triangles) at pH 7.5 (filled symbols) and 8.9 (open symbols). The experimental conditions were as in Fig. 4. k_2 was obtained from a curve-fitting analysis as in Fig. 5, but this time the apparent rate constants of the fastest and slowest phases, k_1 and k_3, were kept fixed at the average values obtained in the analysis for Fig. 5. The dashed curves are hyperbolic functions that best fit the k_2 points. Characteristic parameters of the hyperbolae are given in Table 1.

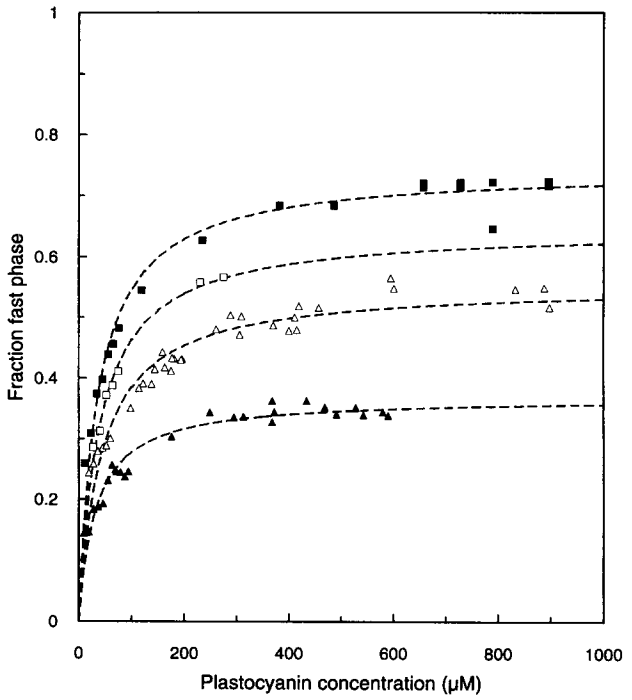

Fig. 7. Effect of Pc concentration on the fraction of the fast phase, defined as the amplitude ratio $A_1/(A_1 + A_2)$ in the text, in the decay kinetics of oxidized P700 for Pc(WT) (squares) and Pc(Y83H) (triangles) at pH 7.5 (filled symbols) and 8.9 (open symbols). The experimental conditions were as in Fig. 4 and the amplitudes of the fast and intermediary decay components, A_1 and A_2, were obtained from a curve-fitting analysis as in Fig. 6. The characteristic parameters of the hyperbolic functions (dashed curves) are given in Table 1.

4. Discussion

The pK^* value of 8.44 reported here for His-83 in the Pc(Y83H) mutant compares well with those obtained from the pH dependence of the oxidation kinetics of the same mutant with $[Fe(CN)_6]^{3-}$ (pK = 7.9) and $[Co(phen)_3]^{3+}$ (pK = 8.4) [8]. This value is unusually high for a protein histidine, in comparison with a pK of 6.90 for the model compound glycyl-L-histidylglycin [23]. A similar result has been reported by Andersson et al. [24], who found an increase in pK of approx. 1.5 pH units for the deprotonation of NO_2-modified Tyr-83 of spinach Pc compared to the model tyrosine tripeptides, which were used as a control. They found an increase in pK values from 7.0 to 8.6 and 8.3 for reduced and oxidized Pc, respectively (values of 8.78 and 8.10 were reported by Christensen et al. [25]).

Assuming no major conformational change in spinach

Pc compared to the crystal structure of poplar Pc, the high pK observed for His-83 in Pc(Y83H) might be understandable. Residue 83 is located in the acidic patch of Pc, surrounded by six acidic residues (Asp or Glu) with their negative charges within 1 nm from the side chain of residue 83 [26]. These charges could stabilize a proton on His-83. In the case of Pc from *Scenedesmus obliquus*, a high pK of 7.8 was found for His-59, a residue which also is located in an acidic surrounding, but this residue is not present in the higher plant plastocyanins [27].

The exchange rate of His-83 corresponds to a lifetime of 100 μs, a value normally found for a freely titrating surface histidine [21]. Residue 83 in Pc is sometimes referred to as partially exposed [28], and one would thus expect a longer lifetime than 100 μs. However, Chothia and Lesk [29] have calculated an accessible surface area of 0.40 nm^2 for Tyr-83 in poplar Pc, thus describing it as an exposed residue. NMR studies on french bean (*Phaseolus vulgaris*) Pc [30] and spinach Pc [31,32], show that the two *ortho* protons of Tyr-83 are equivalent, as are the two *meta* protons, consistent with a relatively large mobility of the side chain of this residue.

The reduction potential of Pc(Y83H) decreases by 29 mV upon deprotonation (Table 1). This is similar to the 20–25 mV decrease observed when NO_2-modified Tyr-83 in spinach Pc is deprotonated [25] (see however [33], where no pH dependence could be observed), but larger than the 7–15 mV decrease that accompanies the deprotonation of His-59 in *S. obliquus* [27]. The large shift observed here can hardly be ascribed to a pure electrostatic interaction since residue 83 is exposed to the solvent, where the dielectric constant is high, and since the distance to the Cu ion is large (approx. 1 nm). However, it is possible that part of the interaction is mediated by structural changes of the protein. This is supported by the findings in [34] which indicate that residue 83 is involved in redox state-dependent conformational changes. The structural change at the Cu site must, however, be small in nature since, in the present work, no effects could be seen in the EPR or optical absorption spectra upon deprotonation of His-83.

The ET from Pc to PS I is slower for Pc(Y83H) than for Pc(WT) (Fig. 4A,C). This was already reported in [4] and an analysis suggested that it was the intracomplex ET rate, k_{et}, that had become slower by the mutation. The earlier kinetic studies have now been extended to include the effect of varying Pc concentrations and elevated pH. This will allow a more quantitative description of the effect of the mutation.

A curve-fitting analysis of the 830 nm absorption transients reveals a complicated behavior. At Pc concentrations above 200 μM there are three exponential decay components while at lower concentrations an additional phase appears. A slow component, ascribed to the reduction of Pc^{ox} by ascorbate [4,9], is always present at an amplitude of 20% of the initial amplitude. The remaining decay components (two at high Pc concentrations and three at low Pc concentrations) are attributed to the reduction of $P700^{ox}$ and they will now be related to possible kinetic models.

Consider first the following model (Scheme 1) in which the intracomplex ET is preceded only by the complex-formation step (determined by the rate constants k_{on} and k_{off}; P stands for P700):

$$Pc^{red} + P^{ox} \underset{k_{off}}{\overset{k_{on}[Pc]}{\rightleftharpoons}} Pc^{red} \cdot P^{ox} \xrightarrow{k_{et}} Pc^{ox} \cdot P^{red}$$

Scheme 1.

At low Pc concentrations ($[Pc] \ll k_{et}/k_{on}$) this scheme would result in two components in the $P700^{ox}$ reduction kinetics with apparent rate constants of $k_1 = k_{et} + k_{off}$ and $k_2 = (k_{et}/k_1)k_{on}[Pc]$ and with an amplitude ratio of $R = (k_{et}/k_1)[Pc]/(K_{diss} + [Pc])$, where $K_{diss} = k_{off}/k_{on}$. At high Pc concentrations ($[Pc] \gg k_{et}/k_{on}$) k_2 would saturate at $k_2 = k_{et}$ while k_1 would increase as $k_1 = k_{on}[Pc] + k_{off}$, but the amplitude of this component would approach zero resulting in a monoexponential decay of $P700^{ox}$.

From the results reported here it is clear that (i) the reduction kinetics of $P700^{ox}$ are biexponential at high Pc concentrations, and — at least — triexponential at low concentrations (< 200 μM); and (ii) the saturating value of k_2, k_{2max}, is far below the value of k_1 (Table 1). The model in Scheme 1 cannot account for these observations and must therefore be discarded as too simple.

The second observation above was also made by Bottin and Mathis [9] and two alternative schemes were put forward, a 'linear' one and a 'parallel' one. The linear scheme includes two conformations of the Pc · PS I complex, with Pc bound in a 'close' (Pc · P) or a 'distant' (Pc · · · P) conformation that are in equilibrium. The close bound state is assumed to be an obligate intermediate in the ET from the distant bound state, i.e., the conformational change constitutes a rate-limiting step (determined by the rate constants k_d and k_c):

$$Pc^{red} + P^{ox} \underset{k_{off}}{\overset{k_{on}[Pc]}{\rightleftharpoons}} Pc^{red} \cdots P^{ox} \underset{k_c}{\overset{k_d}{\rightleftharpoons}} Pc^{red} \cdot P^{ox} \xrightarrow{k_{et}} Pc^{ox} \cdot P^{red}$$

Scheme 2.

This scheme, which is similar to a model used for the ET from cytochrome c_2 to the reaction center in *Rhodobacter sphaeroides* [35–37], can account well for the results presented here and it will be shown that the kinetic data can be used to estimate the rate constants k_c, k_d and k_{et}.

Consider first, however, the parallel scheme of Bottin and Mathis [9]. This was assumed to consist of two different binding sites for Pc on PS I, a 'close' and a 'distant', with Pc reacting at each site according to Scheme 1 but with different rate constants for the two sites. In

particular, the $t_{1/2}$ for ET was suggested to be 12 and 110 μs for the two sites (corresponding to rate constants of $58 \cdot 10^3$ and $6.3 \cdot 10^3$ s^{-1}) [9]. In later double-flash experiments the same workers showed that two Pc molecules can be bound simultaneously to PS I and that the second, 'distant' bound Pc can donate an electron to $P700^{ox}$, either directly, or, via the 'close' bound one with a $t_{1/2}$ of 110 μs [38]. The direct transfer alternative would then correspond to the earlier proposed parallel scheme.

A parallel scheme cannot account for the present findings. At high Pc concentrations, when both sites are occupied, this model would result in a monoexponential decay of $P700^{ox}$, with an apparent rate constant given by the sum of the ET rate constants for the two sites (i.e., $64 \cdot 10^3$ s^{-1}), contrary to the observed biexponential decay. Therefore, the parallel scheme has to be ruled out. However, it is still possible that two Pc molecules can donate electrons to $P700^{ox}$ but then the ET from the 'distant' bound one has to occur via the 'close' bound one in order to obtain consistency between the double-flash experiments [38] and the present results.

Returning to the linear Scheme 2, this model generally gives rise to three phases in the decay kinetics of $P700^{ox}$ but at high Pc concentrations one of these has a zero amplitude. When going from a high to a low Pc concentration, the number of decay components is therefore expected to increase from two to three. This is consistent with the observed behavior. However, it was not possible to resolve the third phase. Instead it made its appearance as an addition to the amplitude of the slow, millisecond, component due to Pc^{ox}. The way in which the slow phase manifests itself depends critically on how the curve-fitting analysis is performed. Here, the apparent rate constant of the slowest phase, k_3, was kept fixed at all Pc concentrations. If, in addition, its amplitude, A_3, was kept fixed, this resulted in a sigmoidal dependence of the apparent rate constant of the intermediary phase, k_2, on the Pc concentration. Such a sigmoidal dependence was reported in [39] and was suggested to reflect a cooperativity in the binding of Pc. The present analysis offers an alternative explanation. However, the complex nature of the $P700^{ox}$ kinetics makes it difficult to draw any firm conclusions about the binding process (i.e., k_{on} and k_{off} in Scheme 2).

Turning to the limit of high Pc concentrations, when the binding site for Pc is saturated, it can be shown from Scheme 2 that the apparent rate constants of the two nonzero components are well approximated by

$$k_1 \approx k_c + k_{et} \quad (4)$$

$$k_2 \approx k_d k_{et}/k_1 \quad (5)$$

and their amplitude ratio by

$$R \approx k_2/(k_c + k_d) \quad (6)$$

These relations have been derived under the assumption that $k_d \ll k_{et}$, i.e., that the conformational change is rate-limiting.

Eqs. (4–6) can be solved for k_c, k_d and k_{et}, and Table 2 lists the values obtained when the experimental estimates k_1, k_{2max} and R_{max} (Table 1) are used in the equations. As seen from Table 2, k_{et} for Pc(Y83H) is less than half the value for Pc(WT) at pH 7.5. When the pH is increased to 8.9, k_{et} for Pc(Y83H) increases with a factor of 1.4. An increase is as expected from the larger driving force at the higher pH, but it is less than the factor of 1.75 that is expected from ET theory [40] if the driving force is the only pH-dependent parameter. Other factors, such as the reorganization energy may, however, contribute.

The rate constants k_d and k_c determine the equilibrium constant K_{dc} $(= k_d/k_c)$ for the conformational change. From Table 2 it is seen that K_{dc} is approx. 1 for Pc(Y83H) at pH 7.5, significantly lower than the value of 4 for Pc(WT). Increasing the pH leads to an increase in K_{dc} for the mutant protein. Thus, the protonation state of the His-83 residue seems to have an influence on the conformational change of the Pc-PS I complex.

In summary, the slower kinetics that are observed for the Pc(Y83H) mutant at the lower pH can be attributed to a dual effect of the protonation of the His-83 residue: (i) A destabilization of the 'close' bound conformation, i.e., the one competent in electron transfer; and (ii) a smaller intracomplex ET rate constant, partly due to a smaller driving force for ET. Since the effects are only relatively

Table 2
Rate constants for wild-type and Tyr83-His plastocyanin mutants calculated assuming that the electron transfer to P700 is preceded by a conformational change of the plastocyanin-Photosystem I complex

Plastocyanin	pH	E^0 (mV)	k_d (10^3 s^{-1})	k_c (10^3 s^{-1})	k_{et} (10^3 s^{-1})
Wild type	7.5	384	20	5	69
Wild type	8.9	388	22	8	67
Tyr83-His	7.5	419	9	10	31
Tyr83-His	8.9	390	14	8	43

The rate constants k_c, k_d and k_{et}, defined in the kinetic Scheme 2 in the text, were calculated from the experimental estimates k_1, k_{2max} and R_{max} (Table 1), using Eqs. (4–6) in the text.

small and indirect, it is concluded that the Tyr-83 residue is not a part of the ET pathway to PS I.

Acknowledgements

We thank Professors Harry B. Gray, Bo G. Malmström and Tore Vänngård and Dr. Thomas Nilsson for valuable discussions. We also thank Mr. Simon Young for help with the protein production and purification and Dr. Roland Aasa for assistance with obtaining the EPR spectra. This work was supported by the Swedish Natural Science Research Council.

References

[1] Haehnel, W. (1986) in Encyclopedia of Plant Physiology, Vol. 19, pp. 547–559, Springer, Berlin.
[2] Colman, P.M., Freeman, H.C., Guss, J.M., Murata, M., Norris, V.A., Ramshaw, J.A.M. and Venkatappa, M.P. (1978) Nature 272, 319–324.
[3] Sykes, A.G. (1991) Structure and Bonding 75, 175–224.
[4] Nordling, M., Sigfridsson, K., Young, S., Lundberg, L.G. and Hansson, Ö. (1991) FEBS Lett. 291, 327–330.
[5] Haehnel, W., Jansen, T., Gause, K., Klösgen, R.B., Stahl, B., Michl, D., Huvermann, B., Karas, M. and Herrmann, R.G., (1994) EMBO J. 13, 1028–1038.
[6] He, S., Modi, S., Bendall, D. S. and Gray, J. C. (1991) EMBO J. 10, 4011–4016.
[7] Modi, S., Nordling, M., Lundberg, L.G., Hansson, Ö. and Bendall, D.S. (1992) Biochim. Biophys. Acta 1102, 85–90.
[8] Kyritsis, P., Dennison, C., McFarlane, W., Nordling, M., Vänngård, T., Young, S., and Sykes, A.G. (1993) J. Chem. Soc. Dalton Trans. 2289–2296.
[9] Bottin, H. and Mathis, P. (1985) Biochemistry 24, 6453–6460.
[10] Nordling, M., Olausson, T. and Lundberg, L.G. (1990) FEBS Lett. 276, 98–102.
[11] Landt, O., Grunert, H.-P. and Hahn, U. (1990) Gene 96, 125–128.
[12] Maurer, R., Meyer, B.J. and Ptashne, M. (1980) J. Mol. Biol. 139, 147–161.
[13] Katoh, S., Shiratori, I. and Takamiya, A. (1962) J. Biochem. 51, 32–40.
[14] Boardman, N.K. (1971) Methods Enzymol. 23, 268–276.
[15] Takabe, T., Ishikawa, H., Niwa, S. and Tanaka, Y. (1984) J. Biochem. 96, 385–393.
[16] Malkin, R. and Bearden, A.J. (1973) Biochim. Biophys. Acta 292, 169–185.
[17] Lockau, W. (1979) Eur. J. Biochem. 94, 365–373.
[18] Olsen, L.F. and Cox, R.P. (1982) Biochim. Biophys. Acta 679, 436–443.
[19] Hoganson, C.W., Casey, P.C. and Hansson, Ö. (1991) Biochim. Biophys. Acta 1057, 399–406.
[20] Driscoll, P.C., Hill, H.A.O. and Redfield, C. (1987) Eur. J. Biochem. 170, 279–292.
[21] Sudmeier, J.L., Evelhoch, J.L. and Jonsson, N.B.-H. (1980) J. Magn. Reson. 40, 377–390.
[22] Setif, P. and Mathis, P. (1980) Arch. Biochem. Biophys. 204, 477–485.
[23] Markley, J.L. (1975) Acc. Chem. Res. 8, 70–80.
[24] Anderson, G.P., Draheim, J.E. and Gross, E.L. (1985) Biochim. Biophys. Acta 810, 123–131.
[25] Christensen, H.E.M., Ulstrup, J. and Sykes, A.G. (1990) Biochim. Biophys. Acta 1039, 94–102.
[26] Guss, J.M. and Freeman, H.C. (1983) J. Mol. Biol. 169, 521–563.
[27] McGinnis, J., Sinclair-Day, J.D., Sykes, A.G., Powls, R., Moore, J. and Wright, P.E. (1988) Inorg. Chem. 27, 2306–2312.
[28] Durell, S.R., Labanowski, J.K. and Gross, E.L. (1990) Arch. Biochem. Biophys. 277, 241–254.
[29] Chothia, C. and Lesk, A.M. (1982) J. Mol. Biol. 160, 309–323.
[30] Freeman, H.C., Norris, V.A., Ramshaw, J.A.M. and Wright, P.E. (1978) FEBS Lett. 86, 131–135.
[31] Driscoll, P.C., Hill, H.A.O. and Redfield, C. (1987) Eur. J. Biochem. 170, 279–292.
[32] Chazin, W.J. and Wright, P.E. (1988) J. Mol. Biol. 202, 623–636.
[33] Gross, E.L. and Curtiss, A. (1991) Biochim. Biophys. Acta 1056, 166–172.
[34] Gross, E.L., Anderson, G.P., Ketchner, S.L. and Draheim, J.E. (1985) Biochim. Biophys. Acta 808, 437–447.
[35] Dutton, P.L. and Prince, R.C. (1978) in The Photosynthetic Bacteria (Clayton, R.K. and Sistrom, W.R., eds.), pp. 525–570, Plenum Press, New York.
[36] Overfield, R.E., Wraight, C.A. and DeVault, D. (1979) FEBS Lett. 105, 137–142.
[37] Tiede, D.M. and Chang, C.-H. (1988) Isr. J. Chem. 28, 183–191.
[38] Bottin, H. and Mathis, P. (1987) Biochem. Biophys. Acta 892, 91–98.
[39] Hervás, M., de la Rosa, M.A. and Tollin, G. (1992) Eur. J. Biochem. 203, 115–120.
[40] Marcus, R.A. and Sutin, N. (1985) Biochim. Biophys. Acta 811, 265–322.